Chem Soc Rev

This article was published as part of the

2008 Chemistry at Surfaces issue

Reviewing the latest developments in surface science

All authors contributed to this issue in honour of the 2007 Nobel Prize winner Professor Gerhard Ertl

Please take a look at the issue 10 table of contents to access the other reviews

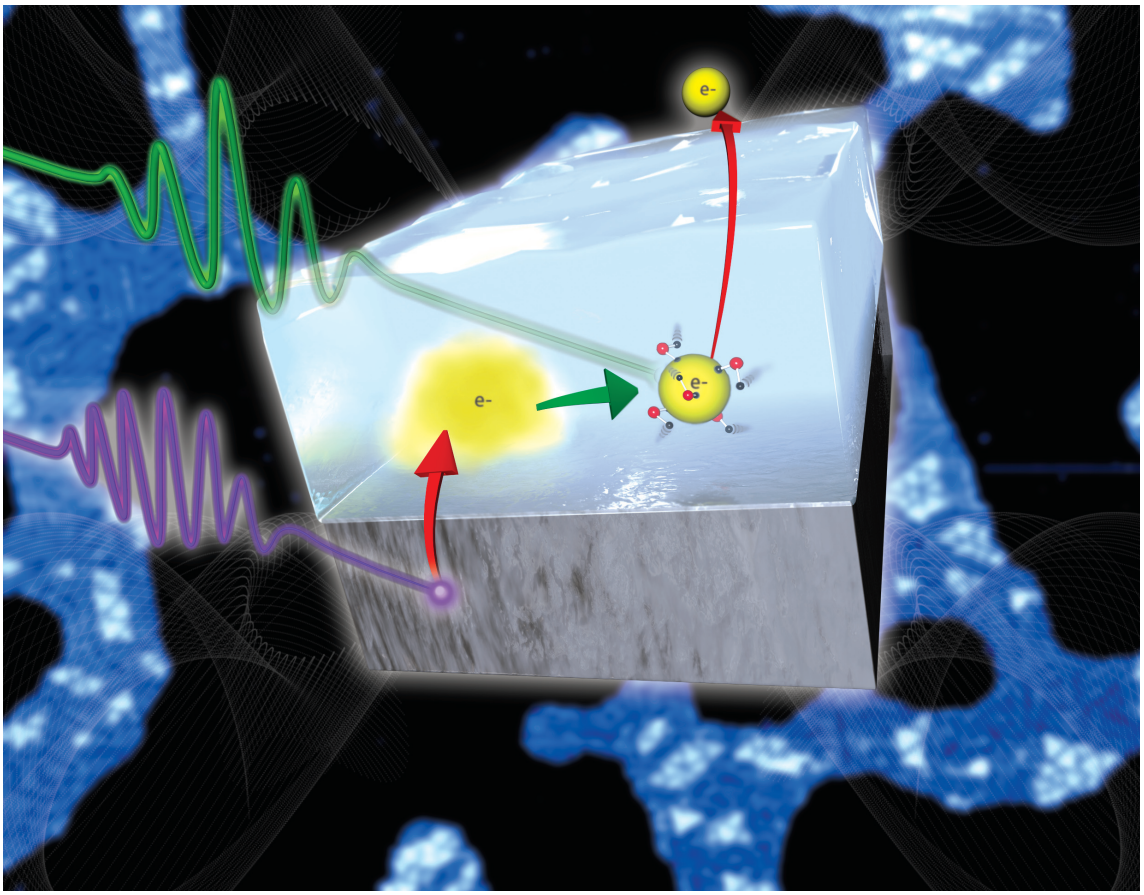

Catalytic reaction energetics by single crystal adsorption calorimetry: hydrocarbons on Pt(111)†

Ole Lytken, Wanda Lew and Charles T. Campbell*

Received 30th June 2008
First published as an Advance Article on the web 18th August 2008
DOI: 10.1039/b719543p

Single crystal adsorption calorimetry provides essential information about the energetics of surface reactions on well-defined surfaces where the adsorbed reaction products can be clearly identified. In this *tutorial review*, we cover the essentials of that technique, with emphasis on our lab's recent advances in sensitivity and temperature range, and demonstrate what can be achieved through a review of selected example studies concerning adsorption and dehydrogenation of hydrocarbons on Pt(111). A fairly complete reaction enthalpy diagram is presented for the dehydrogenation of cyclohexane to benzene on Pt(111).

I. Introduction

Highly skilled organic chemists are able to design reactions and entire synthetic schemes based on their knowledge of the bond strengths in and relative thermodynamic stabilities of the reaction intermediates involved. Chemists studying heterogeneous catalysis and surface chemistry are decades behind in this respect, due to their general lack of knowledge of bond energies of species adsorbed to surfaces and their relative thermodynamic stabilities. A crucial role has been played by calorimetric measurements in advancing organic and inorganic chemistry to their current state. The whole basis for fundamentally understanding reactivity trends in organic and inorganic chemistry lies in their strong thermodynamic underpinnings as revealed by calorimetry. In this sense, surface chemistry is far behind.

Department of Chemistry, University of Washington, Seattle, Washington 98195-1700, USA.
E-mail: campbell@chem.washington.edu

† Part of a thematic issue covering reactions at surfaces in honour of the 2007 Nobel Prize winner Professor Gerhard Ertl.

Already in the early days of surface chemistry, calorimetric measurements of heats of adsorption of gases on high surface area metal films were being performed (ref. 1 and 2 and references therein). However, on such complex surfaces, it is generally not clear what are the structures or even the chemical formulas of the adsorbates being formed upon gas adsorption. Ertl,[3–5] Somorjai[6] and others pioneered the study of catalytic reaction mechanisms using single crystal surfaces as model catalysts, showing that these much simpler surfaces offer tremendous advantages in that they allow much easier determination of the chemical formulas and even geometric structures of the adsorbates formed upon gas adsorption. Subsequent studies showed that elementary reaction steps have different rate constants and activation energies on different single crystal facets of the same metal, so that kinetic studies are also greatly simplified when performed on a single crystal surface. Thus, for adsorption calorimetry to be most powerful, it must be done on single crystal surfaces.

Surface chemists have for decades measured adsorption energies using temperature programmed desorption (TPD) and equilibrium adsorption isotherms, but these techniques only work for adsorbed species that are completely reversibly

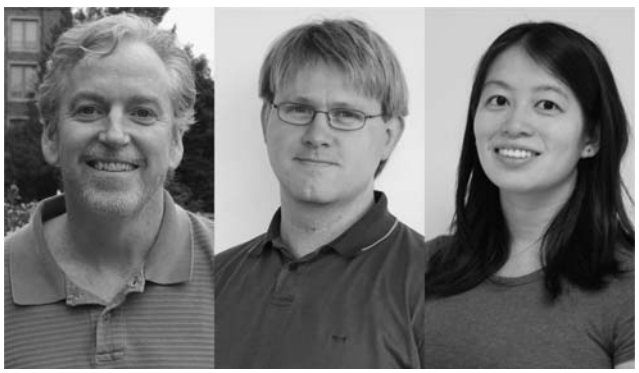

Charles T. Campbell, Ole Lytken and Wanda Lew

Charles T. Campbell received his PhD from the University of Texas at Austin with J. M. White. He did postdoctoral research in Munich with Gerhard Ertl and was a staff scientist at Los Alamos National Lab. He is the Lloyd E. and Florence M. West Professor of Chemistry at the University of Washington. He has received the Arthur W. Adamson Award of the American Chemical Society (ACS), its Award for Colloid or Surface Chemistry, an Alexander von Humboldt Research Award and the Yarwood Award of the British Vacuum Council. He is Editor-in-Chief of Surface Science and was Chair of the ACS Colloid/Surface Chemistry Division. He studies surface science, catalysis and bioanalytical chemistry. Ole Lytken received a PhD degree from the Technical University of Denmark and is a Postdoctoral Associate with Campbell. Wanda Lew received her BA degree from the University of California at Berkeley and is a PhD student with Campbell.

desorbed. While in many cases TPD can provide a desorption activation energy that is equal to the isosteric heat of adsorption (minus $1/2RT$), often the adsorbate cannot be desorbed intact and will predominantly dissociate during TPD. Furthermore, many catalytically-interesting adsorbates transform into higher-temperature structures before reaching the temperature at which they desorb. Finally, the substrate may decompose or restructure during heating before the adsorbate desorbs. Thus, in many cases, TPD cannot provide heats of adsorption for the species of interest. For similar reasons, equilibrium adsorption isotherms are also of limited value in this respect. Thus, there is a tremendous need for direct calorimetric measurements of adsorption energies on single crystal surfaces.

In the mid 1980s, Richard Masel's group developed the first calorimeter that could measure adsorption energies on single crystals,[7] but noise problems limited its precision, and so it proved to have little impact on understanding surface chemistry. It did, however, introduce the importance of using very thin single crystals, and highlighted the key problematic issues which needed further invention. In ~1990, David King and his group at Cambridge University developed an apparatus for adsorption microcalorimetry that could work on single crystal surfaces with sufficient precision to make important contributions to our understanding of the energetics of surface reactions.[8–11] Referring to this as "single crystal adsorption calorimetry", or SCAC, King's group more recently showed that measurements could be made as a detailed function of coverage with a detection limit of ~10 kJ mol^{-1} and an absolute accuracy of ~6%.[12] King's preferred method for heat detection relies on ultrathin (200 nm) metal single crystals whose transient temperature rise after adsorption of a pulse of gas containing ~5% of a monolayer is measured with infrared optical pyrometry. This single crystal adsorption calorimeter from King's group is already making a big impact on our understanding of the energetics of surface reactions.[13–19]

Our group recently developed a new method for single crystal adsorption calorimetry.[20–26] It is partially based on King's method above, but uses a novel pyroelectric polymer heat detector which has several advantages over previous designs, including the abilities to (1) more easily prepare the single crystal sample surface since the detector is completely detached from the crystal while its surface is being prepared, (2) use much thicker samples, since the sensitivity is ~400 times better; hence, much smaller temperature changes can be detected, (3) use a wider variety of substrates, and (4) measure at much lower temperatures (down to 100 K or less). Here we present a tutorial review on how this calorimeter operates and the types of information that it provides. We emphasize particularly the insights it has provided regarding the catalytic dehydrogenation and hydrogenation of hydrocarbons on Pt(111) model catalysts. We show too that such accurate calorimetric measurements can also provide benchmarks against which to compare various approximate theoretical methods for calculating adsorption energies.

King's group also first introduced the concept of using a pyroelectric material touching the sample as a heat detector for low-temperature calorimetry,[27] but in their case a rigid inorganic crystal (lithium niobate) was used as the detector, so it had to be fused to the sample. Since this detector has an upper temperature limit which is too low to allow annealing of most single crystal materials to high enough temperatures to get an ordered surface, it has limited applicability. It also had a much poorer signal-to-noise ratio than the system described here.

II. Calorimeter design

In the calorimeter design developed by our group,[20–24,26] a pulse of gas from a 4 mm diameter molecular beam strikes the surface of a single crystal sample, mounted in an ultrahigh vacuum surface analysis chamber. The heat released from the adsorption of each gas pulse is measured by gently pressing a thin pyroelectric polymer ribbon against the back side of the single crystal sample. Fig. 1 shows a typical ribbon mounted on its holder so that it can be translated into the back of the crystal. The ~50 mm × 4 mm ribbon is cut from a 9 μm thick, uni-axially oriented β-polyvinylidene fluoride (PVDF) polymer sheet, coated on the front and back faces with thin Al films, which are connected to an external preamplifier. A temperature change in the pyroelectric polymer releases an electrical charge into the preamplifier, detected as a voltage pulse across a 10 GΩ resistor.

Each gas pulse contains the same amount of gas, typically 1% of a monolayer (ML) depending on the gas; one ML is defined here as one adsorbate molecule per surface atom. (Below, we define coverage, θ, in these same ML units throughout.) Upon adsorption, approximately 200 nJ of heat is typically released to the sample (for the 40 kJ mol^{-1} heat of adsorption of multilayer cyclohexene), corresponding to an ~8 mK temperature change in a sample with a typical thickness of 1 μm and the heat capacity of Pt. The corresponding temperature change in the pyroelectric polymer is only

Fig. 1 Pyroelectric heat detector and its holder. The 4 mm-wide pyroelectric polymer ribbon, in the form of an arch, protrudes from this conical holder designed to fit exactly into the conical recess in the mating sample holder for the single crystal, so that the flexible ribbon compresses against the back surface of the crystal, deforming inward by a fixed amount (~2 mm) and simultaneously flattening across the crystal's surface. This holder is cooled by Cu braids which attach to a gas-cooled Cu reservoir, and can be stabilized at temperatures down to 100 K. It is retracted from the sample holder (by translating to the left), so that the sample holder can be moved to different parts of the chamber for surface analysis, cleaning or annealing.

$\sim$0.3 mK. Mounting the pyroelectric ribbon so that it presses harder against the sample when in contact improves the heat transfer, but at the risk of deforming the crystal. At low temperature the polymer is stiffer, thus increasing piezoelectric noise pickup from vibrations, and thermal drift is more difficult to control, so the signal-to-noise ratio is lower. However, even at 100 K we achieved a typical pulse-to-pulse standard deviation for the adsorption of cyclohexene on Pt(111) of 15 nJ, corresponding to 2.5 kJ mol^{-1} or 6% of the deposited energy per pulse for multilayer adsorption (40 kJ mol^{-1}). In the best runs, this was as low as 1.2 kJ mol^{-1}. To reduce noise and prevent shorts across the pyroelectric ribbon at low temperatures, the aluminium coating on the PVDF ribbon was removed except in a patterned area essential for measurement. This also reduces the capacitance of the detector, thus increasing the voltage response.

While the single crystal samples studied with this detector are typically 1 μm thick, we have used this same basic detector design to measure adsorption energies on crystals as thick as 80 μm with acceptable signal-to-noise.[25] Sensitivity improvement is needed for measuring such thick samples. It is achieved by increasing the compression between the single crystal and the thin PVDF detector ribbon by pressing it to the sample with a thicker, insulating polymer, and by using a similarly-mounted reference detector to subtract away some of the voltage noise due to mechanical vibrations (also detected as a current by the piezoelectric PVDF ribbon). This system can measure heats on single crystal samples that are $\sim$400 times thicker than those used in King's calorimeter with similar signal-to-noise in units of kJ mol^{-1}. Since such thick samples have an $\sim$400-fold lower temperature rise for a given heat input, this really means that this heat detector's sensitivity is $\sim$400 times better. This broadens the range of surfaces that can be studied by calorimetry, since this thickness of 80 μm can be achieved with nearly any single crystal material by simple mechanical thinning, whereas that is not possible with samples thinner than $\sim$50 μm over the required surface area of $\sim$1 cm^2.

Since the coverage resolution of this apparatus is $\sim$0.01 ML, it will measure the energy to form a single adsorbed species, if one forms in any narrow coverage range, and even measure adsorption energies at defects present only at very low concentration if preferentially populated at low coverage. Identifying the structure and nature of the species being formed on the surface is not the subject of this review, but it can usually be done using existing surface structural characterization techniques. Such structural characterization is necessary in order for the results with this apparatus to be of the greatest utility. Indeed, it is best to choose systems to study with calorimetry which have already been studied in detail with other surface science techniques, so that the species being created are known.

Fig. 2 shows a low-energy electron diffraction (LEED) surface crystallography pattern of a 1 μm-thick Pt(111) single crystal after extensive use in calorimetry. The sharp Bragg diffraction spots (small bright spots) demonstrate the lasting quality of the single-crystalline surface order. This figure also shows some details of the Pt crystal's mounting on the end of an ultrahigh vacuum manipulator.

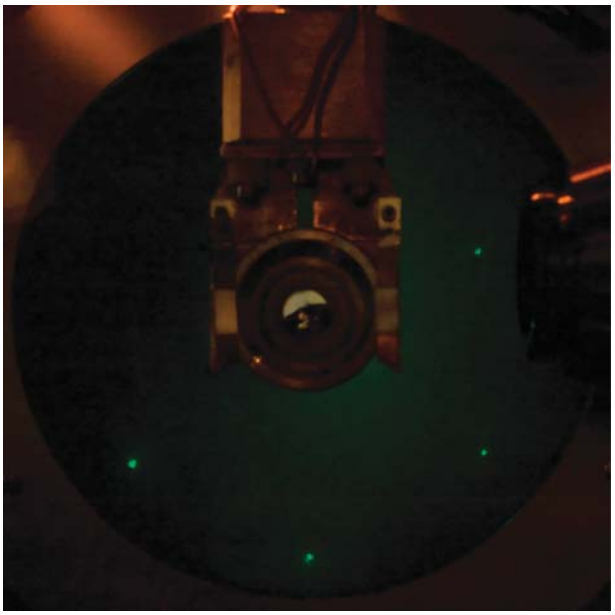

Fig. 2 LEED pattern at 73 eV beam energy of a 1 μm-thick Pt(111) single crystal after use in calorimetry measurements, showing its sharp Bragg diffraction spots. Also apparent is the sample platen manipulator fork holding a sample platen with its conical recess and hole, covered by the Pt single crystal at its center. This recess aligns the conical heat detector holder (see Fig. 1) so that its pyroelectric ribbon contacts the back of the Pt single crystal through this hole. The (0,0) reflex is hidden by the bottom of the sample platen near the center of the image. The spot at $\sim$10 o'clock is too weak to see in this photo due to a local defect in the LEED screen's fluorescent coating there.

III. Energetics of hydrocarbon adsorption and reactions on Pt(111)

Platinum is used to catalyze many hydrocarbon hydrogenation and dehydrogenation reactions. As the simplest examples of catalytic aromatization, the dehydrogenation of cyclohexane and cyclohexene into benzene over platinum have been very widely studied. Since Pt(111) is the most stable facet of Pt, it has been a key model catalyst used in such studies. We use this as a prototypical catalytic reaction system to show the powerful types of insight that can be gained in our understanding of heterogeneous reaction systems in general, and hydrocarbon conversion reactions catalyzed by Pt more specifically, from the energetics provided by SCAC.

Both cyclohexane and cyclohexene adsorb intact on Pt(111) at temperatures below 150 K.[28–34] Adsorbed cyclohexane dehydrogenates to form adsorbed di-σ-bonded cyclohexene plus $2H_{ad}$ when heated to $\sim$200–250 K (depending on the heating rate and coverage), but some of it desorbs intact. At $\sim$200–250 K adsorbed cyclohexene loses an allylic H to form H_{ad} plus adsorbed c-C_6H_9, a 2-cyclohexenyl species with π-allyl character,[30,33,34] which above $\sim$280 K dehydrogenates further into benzene plus H_{ad}.[28–34] At $\sim$500 K, the adsorbed benzene dehydrogenates further *via* an intermediate with a 2 : 1 C : H ratio, which eventually forms graphitic carbon.[28,29,35] Both the adsorbed cyclohexene and benzene partially desorb intact when heated, in kinetic competition with their dehydrogenation, but only if at high coverage (>60% of

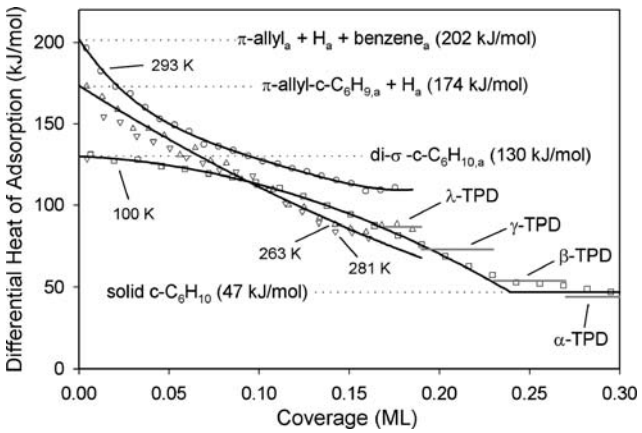

Fig. 3 The differential heat of adsorption of cyclohexene on Pt(111) *versus* coverage, measured at several temperatures in the range from 100 to 293 K, from ref. 26. Shown in the figure as horizontal bars are also the high-coverage adsorption energies estimated based on Redhead analysis of TPD peak temperatures, as reported by Rodriguez and Campbell.[28] At lower coverages, 100% of the adsorbed cyclohexene dissociates during TPD, necessitating these calorimetry measurements.

a saturated monolayer). The heats of formation of several of these isolatable catalytic intermediates between cyclohexene and benzene have been measured using SCAC on Pt(111).[26,36]

The heat of adsorption of cyclohexene on Pt(111) was measured as a function of coverage in the temperature range from 100 K to 300 K,[26] as shown in Fig. 3. At 100 K, cyclohexene adsorbs as intact di-σ-bonded cyclohexene on Pt(111) and the heat of adsorption was found to decrease with coverage, θ, as $(130 - 47\theta - 1250\theta^2)$ kJ mol^{-1}, with an initial heat of adsorption of 130 kJ mol^{-1}. From this, a standard enthalpy of formation of adsorbed di-σ-cyclohexene of −135 kJ mol^{-1} at low coverage was found, starting from the well-known standard enthalpy of formation of gas-phase cyclohexene (−5 kJ mol^{-1})[37]: (−5 − 130) kJ mol^{-1} = −135 kJ mol^{-1}. At 281 K, cyclohexene dehydrogenates upon adsorption, forming adsorbed 2-cyclohexenyl (π-allyl-c-C$_6$H$_9$) plus a hydrogen adatom, and the heat of adsorption was found to decrease with coverage as $(174 - 700\theta + 761\theta^2)$ kJ mol^{-1} with an initial heat of adsorption of 174 kJ mol^{-1}. From this, a standard enthalpy of formation of adsorbed π-allyl-c-C$_6$H$_9$ of −143 kJ mol^{-1} at low coverage was estimated,[26] starting again from gas-phase cyclohexene and adding half of the adsorption energy of H$_2$ gas to make 2H$_{ad}$ on Pt(111) of ∼72 kJ mol^{-1}:[38–41] (−5 − 174 + 72/2) kJ mol^{-1} = −143 kJ mol^{-1}.

The heat of adsorption of benzene on Pt(111) at 300 K was measured calorimetrically and found to decrease with coverage (θ) as $[197 - 48(\theta/\theta_{max}) - 83(\theta/\theta_{max})^2]$ kJ mol^{-1}, where saturation coverage (θ_{max}) is 2.3×10^{14} molecules cm^{-2}.[36] This gives a standard enthalpy of formation of adsorbed benzene on Pt(111) of −114 kJ mol^{-1} at low coverage (starting from the standard heat of formation of benzene gas, 83 kJ mol^{-1}):[37] (83 − 197) kJ mol^{-1} = −114 kJ mol^{-1}. The probability of benzene adsorbing on Pt(111) per molecular collision with the surface was measured by mass spectrometry, and found to be 0.97 on the clean surface, and to decrease very slowly with increasing coverage. The coverage dependence was fit well by a kinetic model which involves a weakly-adsorbed, mobile precursor to chemisorption, with a ratio of its diffusive hopping rate to its desorption rate of ∼28. Consistent with this, benzene was found to adsorb transiently on the benzene-saturated surface at 300 K with a calorimetric heat of adsorption of ∼68 kJ mol^{-1}.[36]

IV. Cyclohexane dehydrogenation pathway on Pt(111): energetics

Using the standard enthalpies of formation of adsorbed di-σ-bonded cyclohexene, the π-allyl species and benzene on Pt(111) at low coverage extracted from calorimetric measurements, as mentioned above, it is possible to draw a partial energy landscape of the dehydrogenation of cyclohexane to benzene on Pt(111), as shown in Fig. 4. Below we describe the details of how we estimated all the energies and activation barriers presented there.

Calorimetric adsorption energies were used to establish the enthalpies of formation of all of the stable intermediates shown in Fig. 4 for Pt(111) except adsorbed cyclohexane and the hydrogen adatoms. The adsorption energy of H$_2$ gas to make 2H$_{ad}$ of ∼72 kJ mol^{-1} was estimated previously using TPD and other methods.[38–41] The adsorption energy of cyclohexane on Pt(111) has been estimated previously to be 58 kJ mol^{-1} by Rodriguez and Campbell[28] using its TPD peak temperature (236 K) and 1st order Redhead analysis. However, they assumed a pre-exponential factor of 10^{13} s^{-1}. Tait *et al.*[42,43] have found that pre-exponential factors for desorption of alkanes of this size are significantly higher than 10^{13} s^{-1}. Using their results, and assuming that the prefactor for desorption scales exponentially with the standard entropy (S^o) of the gas phase molecule (as expected based on the transition-state-theory analysis by Tait *et al.*[42]), we estimate the desorption prefactor for cyclohexane (S^o = 297.3 J K^{-1} mol^{-1})[44] to be somewhere in between the prefactors measured by Tait *et al.* for propane (S^o = 270.3 J K^{-1} mol^{-1})[37] and *n*-butane (S^o = 309.6 J K^{-1} mol^{-1}).[45] For both propane and *n*-butane, Tait *et al.* find desorption prefactors in the range $10^{14.6}$–$10^{15.7}$ s^{-1}.[43] Re-analyzing Rodriguez and Campbell's cyclohexane TPD data using a pre-exponential factor for desorption of 10^{15} s^{-1} instead of 10^{13} s^{-1}, we find a desorption energy of 67 kJ mol^{-1}, which we think is a better estimate. Using instead the peak temperature from Parker *et al.* (225 K at 3 K s^{-1}),[46] we find a very similar desorption energy (within 2 kJ mol^{-1}). Using this value, and setting it equal to the adsorption enthalpy (*i.e.*, assuming no activation energy barrier to adsorption), we estimate the standard enthalpy of formation of adsorbed cyclohexane on Pt(111) to be −190 kJ mol^{-1} (starting from the standard enthalpy of formation of cyclohexane gas of −123 kJ mol^{-1}).[37]

Above, we described how all the stable energy levels shown in Fig. 4 were determined by starting from known gas-phase enthalpies and going to stable adsorbed intermediates by simply subtracting the appropriate heats of adsorption. We next describe how the activation energy barriers shown in Fig. 4 were estimated.

Henn *et al.*[30] also measured the dehydrogenation rate of adsorbed cyclohexane on Pt(111) relative to its desorption

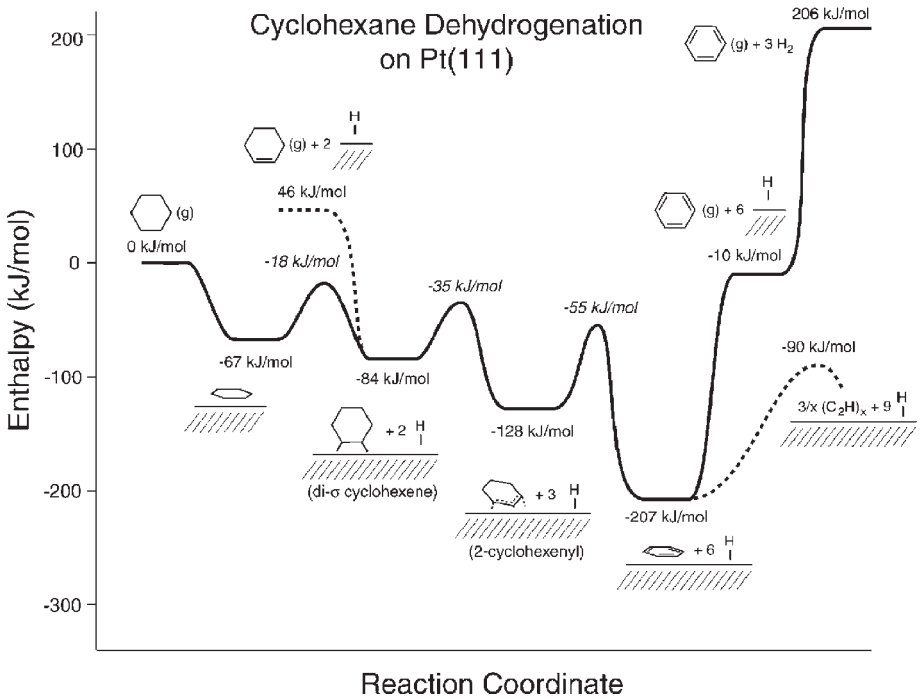

Fig. 4 Reaction enthalpy diagram for cyclohexane dehydrogenation to benzene (and benzene hydrogenation to cyclohexane) over a Pt(111) model catalyst, showing the low-coverage energetics of the key adsorbed intermediates as determined by adsorption microcalorimetry. Also shown are the activation energy barriers for their interconversions determined by a variety of surface reaction kinetic techniques. See text for details.

rate. They found the activation energy for dehydrogenation to be 2 kJ mol^{-1} lower than the barrier for desorption, and the pre-exponential factor for dehydrogenation to be 1.5 times lower than the pre-exponential factor for desorption. Assuming a pre-exponential factor for desorption of 10^{15} s^{-1} (see above), this yields an activation energy barrier for dehydrogenation of cyclohexane on Pt(111) of 65 kJ mol^{-1} with a pre-exponential factor of 7×10^{14} s^{-1}. In another study, Parker *et al.*[46] measured the activation energy barrier for dehydrogenation of cyclohexane on Pt(111) at a coverage of 0.01 ML to be 40 kJ mol^{-1} with a pre-exponential factor of 2×10^{9} s^{-1}, increasing to 49 kJ mol^{-1} and 3.4×10^{11} s^{-1} at 0.03 ML and increasing again to 56 kJ mol^{-1} and 7×10^{12} s^{-1} at 0.06 ML. As a reasonable average, we used here 49 kJ mol^{-1} and 3.4×10^{11} s^{-1}. All values are in agreement with the reported branching ratio between the rates of dehydrogenation and desorption of approximately two at 236 K.[28]

Since the dehydrogenation of cyclohexene to c-C_6H_9 at low coverage on Pt(111) takes place at nearly the same temperature as the dehydrogenation of cyclohexane,[28,30,32–34,46] we assume here that both activation energy barriers are identical (*i.e.*, $\sim$49 kJ mol^{-1}).

This adsorbed 2-cyclohexenyl (π-allyl) species dehydrogenates to form adsorbed benzene at $\sim$300 K (20–80% conversion in 30 s),[33,46] by overcoming an estimated activation energy barrier of $\sim$73 kJ mol^{-1}, assuming a similar prefactor of 10^{11} s^{-1}. This is close to the value of $\sim$87 kJ mol^{-1} estimated from quantitative studies of cyclohexene dehydrogenation *versus* temperature by Henn *et al.*,[30] given the fact that they assumed a larger prefactor of 7.7×10^{12} s^{-1}.

Benzene dehydrogenation has been studied by Campbell *et al.*[35] and has been found to produce H_2 gas in a reaction-limited event with a peak temperature of 535 K at a heating rate of 7 K s^{-1}. Assuming a similar prefactor of 10^{11} s^{-1}, this gives an activation barrier of 117 kJ mol^{-1}.

The dehydrogenation steps mentioned above have been found to exhibit a primary kinetic isotope effect quantitatively consistent with the activation energy being higher for perdeuterated species (relative to non-deuterated) by the full difference between the zero-point vibrational energies of C–D *versus* C–H bonds.[28,35,47] This strongly suggests that C–H cleavage is the rate-determining step, and that the C–H bond is nearly completely broken in the transition state.

Fig. 4 provides some interesting insight into platinum-catalyzed cyclohexane and cyclohexene dehydrogenation, and benzene hydrogenation. It is easy to see why it is difficult to stop dehydrogenating cyclohexane at the olefin product (cyclohexene gas). The barrier for its desorption is much higher than that for its further dehydrogenation. This is also why no benzene gas is produced at low coverages during cyclohexane and cyclohexene dehydrogenation during TPD. The barrier for benzene desorption is simply too high. Indeed, the only way that benzene gas can be produced is for the coverages of coadsorbed species to increase, such that the desorption barrier decreases and the dissociation barrier increases, so that benzene desorption eventually becomes competitive with dissociation. As seen in Fig. 3, the heats of adsorption for all these adsorbates decrease rapidly with increasing coverage, and their corresponding enthalpies of formation increase, thus decreasing their barriers for desorption. At the same time, the free sites needed for C–H cleavage get filled as coverage increases, so that the effective barrier for hydrogen abstraction by Pt sites increases. At the high-pressure, high-coverage conditions of real catalysis, the desorption of dehydrogenated products is thus kinetically

competitive with complete dehydrogenation (which would eventually coke the catalyst).

Bismuth adatoms serve as nearly inert steric site blockers when coadsorbed with hydrocarbons at low coverages of both, and therefore can be used to investigate ensemble effects in surface reactions in the absence of substantial electronic effects. Previously, this group has explored the ensemble (site-size) requirements for the dehydrogenation of adsorbed hydrocarbons (cyclopentane, cyclopentene, cyclohexane, cyclohexene and benzene) on Pt(111) by measuring the variation in the rate of dehydrogenation of adsorbed hydrocarbons with bismuth coverage (θ_{Bi}).[28,29,35,47–50] The rate data whenever the coverages of both the hydrocarbon and the Bi are low and Bi acts as a nearly inert site blocker are the most interesting.[47,50] As shown in Fig. 5, tiny amounts of added Bi dramatically suppress the dehydrogenation rate of the cyclic alkanes, but they do not affect the rate for the cyclic olefins. This can be easily understood from Fig. 4. For the alkane, the activation energy for C–H bond cleavage is only slightly lower than that for its desorption, and the generally lower prefactor for C–H cleavage[51] contributes to make dehydrogenation have a rate constant that is almost equal to its desorption rate constant (actually in $\sim$1 : 2 ratio at the peak temperature for desorption[28]). Thus, when an alkane is on the surface and heated to the temperature where it will either desorb or dehydrogenate, it has few chances to diffusively visit sites on the surface to find a region where the local Bi coverage is low enough to allow H abstraction by free Pt sites. Once it tries to dehydrogenate in one region, it likely desorbs. In contrast, for the olefin, the barrier for C–H cleavage is far below that for desorption, so the rate constant for dehydrogenation far exceeds that for desorption. Thus, the molecule can make many aborted attempts to dehydrogenate in regions of the surface that are too blocked by Bi before it finally finds a Bi-free region where it can dehydrogenate. Its relative rate of desorption is so slow that it is not kinetically competitive until the Bi coverage is very high.

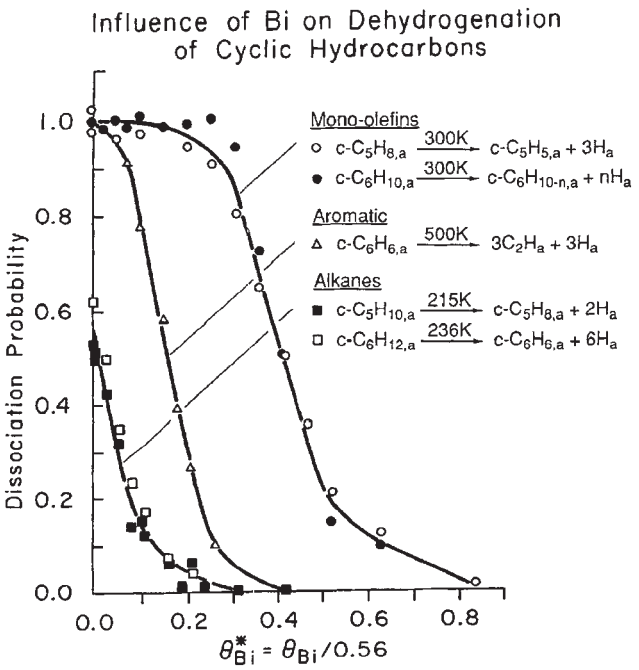

Fig. 5 The dissociation probability for various adsorbed hydrocarbons on Pt(111) *versus* the precoverage of bismuth adatoms, from ref. 50. The probability was measured by TPD, as the fraction of adsorbed species that dissociate (as opposed to desorbing intact) in the limit of low hydrocarbon coverage. Lines through the data represent site-blocking kinetic models described in ref. 47 and 50. Bismuth coverages are relative to its closest-packed monolayer, such that 0.20 on this scale corresponds to only one Bi adatom for every nine surface Pt atoms.

For benzene, the difference in activation barriers for C–H cleavage *versus* desorption ($\sim$80 kJ mol^{-1}) is closer to that for olefins (Fig. 4), yet, the effect of Bi site blocking is intermediate between olefins and alkanes (Fig. 5). We speculate that this may be due to coadsorbed Bi having a more repulsive lateral interaction with low coverages of coadsorbed benzene than for the alkanes and olefins. This would naturally be the case since benzene has a much larger footprint on the surface and therefore sits closer, on average, to Bi adatoms. Furthermore, a dominant bonding mechanism for benzene to Pt may be associated with London dispersion forces (see below), which are probably more easily influenced by coadsorbed Bi (and its associated dipole moment) than are the C–Pt bonds in, for example, di-σ-bonded cyclohexene. When just enough Bi (θ = 0.03) was coadsorbed with a low coverage of adsorbed benzene to suppress dehydrogenation enough to get some observable molecular desorption of the benzene, its TPD peak was seen at $\sim$505 K.[35] This corresponds to a desorption/adsorption enthalpy of only $\sim$130 kJ mol^{-1} for benzene using the same Redhead analysis as in ref. 35. The integral heat of adsorption of pure benzene at this same benzene coverage on Pt(111) is $\sim$170 kJ mol^{-1},[36] $\sim$40 kJ mol^{-1} higher. This comparison suggests that there is $\sim$40 kJ mol^{-1} of repulsive interaction energy on benzene due to the coadsorbed Bi even at this low Bi coverage.

V. Average C–Pt bond energies

Using the measured low-coverage adsorption energy of di-σ-bonded cyclohexene on Pt(111) mentioned above, we have estimated an average C–Pt σ-bond strength of 205 kJ mol^{-1} for di-σ-bonded cyclohexene on Pt(111).[26] This estimate was made by using the thermodynamic cycle shown in Fig. 6, recognizing that the enthalpies in any such cycle must sum to zero. This sum rule, together with all the other steps' enthalpies, gave the value of 409 kJ mol^{-1} shown for the step where two C–Pt σ-bonds are made by attaching the gas-phase diradical to the Pt surface.[26] Dividing this 409 kJ mol^{-1} by two gives their average C–Pt σ-bond energy of 205 kJ mol^{-1}. This bond energy is slightly weaker than the values found by King's group for di-σ-bonded ethylene at moderate coverage on Pt(110)-(1 × 2) (235 kJ mol^{-1})[10] and Pt(100)-(1 × 1) (253 kJ mol^{-1}).[15] This is not caused by the differences in coverages studied, since higher coverages result in even lower adsorption energies. It may be caused by the larger amount of strain in the adsorbed di-σ-bonded cyclohexene molecule, relative to gas phase cyclohexene[52] compared to the case of ethylene, or the lower degree of coordinative unsaturation of the Pt atoms on this (111) face compared to (110) and (100). A small part of this difference is also expected because adsorbed cyclohexene

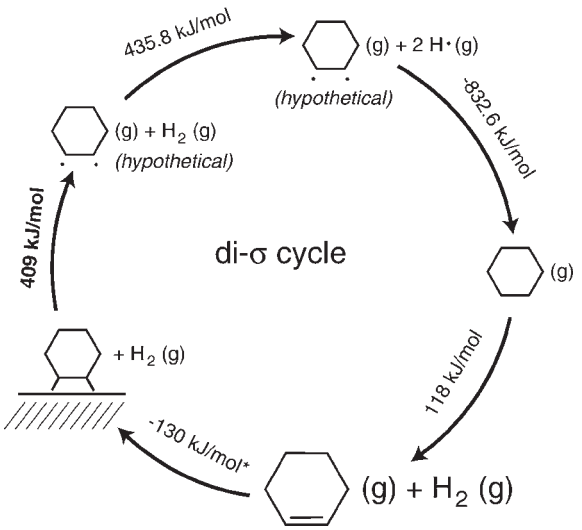

Fig. 6 The thermodynamic cycle used to calculate the average C–Pt bond enthalpy for di-σ-bonded cyclohexene on Pt(111). The value indicated with an * is the standard enthalpy of adsorption from calorimetry, and the value in bold is the adsorption enthalpy, relative to the corresponding gas-phase di-radical, calculated by setting the sum of the enthalpies for that cycle equal to zero. The di-radical is a hypothetical species wherein the energy costs for removing the 2nd hydrogen were assumed to be identical to that for removing the first hydrogen (*i.e.*, the well-known C–H bond energy in gas-phase cyclohexane of 416.3 kJ mol^{-1} [37]). Note that this is exactly the appropriate species to use in estimating the average bond energy here.

involves C–Pt bonds to secondary carbon atoms and not to primary carbon atoms as in adsorbed ethylene (see below).

For organometallic compounds, the bond strength between a ligand and the metal center has been found to scale linearly (with a slope of one) with the bond strength between the same ligand and hydrogen.[53,54] It has also been shown that this correlation may extend at least to a few surface species bonded to bismuth atoms.[55] Fortunately, H–C bond energies are already thoroughly tabulated for many organic functional groups.[37,56] Using these, and assuming that this correlation holds approximately, allows one to use the bond energies measured with SCAC to make rough estimates of many other bond energies. For example, the Pt–C bond energy of $\sim$250 kJ mol^{-1} estimated by King *et al.* for the C atoms of di-σ-bonded ethylene at moderate coverage on Pt(110)-(1 × 2) and Pt(100) can be used to predict the other Pt–C surface bond energies shown in Table 1,[54] in the absence of ring-strain and steric effects of the types mentioned just above.

The above-mentioned 1 : 1 correspondence between these H–C bond energies and M–C bond energies gives strong predictability, provided the value of the metal–C bond energy for any one such group is available. This can be used to real advantage by surface chemists, provided it is recognized that it only predicts the contribution to the adsorption energy of this group from that specific two-center bond. Any additional bonding from other parts of the attached group, for example through π-interactions or agostic bonding by other parts of the organic adsorbate at other sites on the metal surface, is ignored. Differential steric and strain effects are also ignored.

Table 1 Estimated Pt–C surface bond energies based on the corresponding H–C bond energy and the Pt–C bond energy of 250 kJ mol^{-1} (in bold) measured for di-σ-bonded ethylene on Pt(100) and (110) surfaces, following ref. 54

H–C bond type	H–C bond energy/kJ mol^{-1}	Pt–C bond energy/kJ mol^{-1}
H–carbonyl	364	203
H–benzyl	368	207
H–i-C_3H_7	398	237
H–ethyl	411	**250**
H–methyl	440	279
H–vinyl	460	299
H–phenyl	464	303
H–C≡C	552	391

The heat of adsorption of naphthalene on Pt(111) at 300 K was measured with SCAC and found to decrease with coverage, θ, as $(317 - 42(\theta/\theta_{max}) - 128(\theta/\theta_{max})^2)$ kJ mol^{-1}, where the saturation coverage, θ_{max}, corresponds to 1.55×10^{14} molecules cm^{-2}.[57] This includes contributions from adsorption on defect sites at very low coverage, where the adsorption heat was estimated to be $\sim$330 kJ mol^{-1}. After removing defect contributions, the heat of adsorption on the ideal, defect-free surface was estimated to be $(300 - 34\Theta - 199\Theta^2)$ kJ mol^{-1}. From this, a standard enthalpy of formation of adsorbed naphthalene on ideal Pt(111) terraces at low coverage of -149 kJ mol^{-1} was found. Naphthalene was found to adsorb transiently on top of chemisorbed naphthalene molecules with a heat of adsorption of $\sim$85 kJ mol^{-1}.[57]

From the benzene and naphthalene adsorption energies on Pt(111) mentioned above, a Pt–C bond energy of $\sim$30 kJ mol^{-1} per C atom was estimated for aromatic hydrocarbons lying flat on Pt(111) at low coverages.[57] This value drops slightly (to 27 kJ mol^{-1}) at the highest coverage where each molecule can sit in the same site, as shown in Fig. 7. Notice

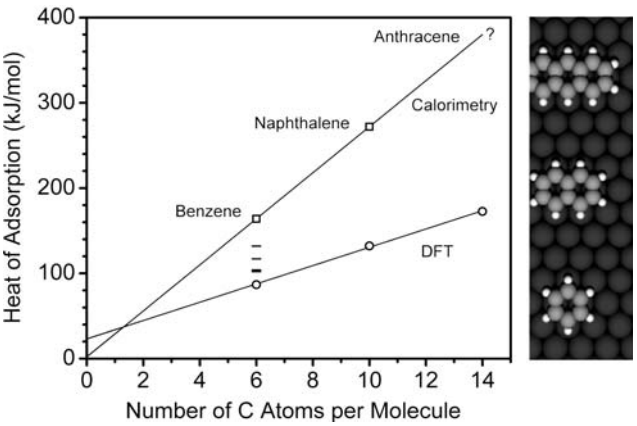

Fig. 7 Comparison of the experimental integral heats of adsorption of benzene and naphthalene on Pt(111) (squares) with computational estimates (circles) at the same coverages (for each case, the highest coverage where all the molecules can sit in the same sites without steric overlap). The lines are the best linear fits of the respective data sets and follow the equations $(11n_C + 23)$ kJ mol^{-1} for DFT and $(27n_C + 2)$ kJ mol^{-1} for calorimetry (with the number of C atoms, n_C). The slope (27 kJ mol^{-1} here) gives the average Pt–C bond energy for aromatic hydrocarbons on Pt(111). The horizontal bars show other computed benzene adsorption energies using different methods. From ref. 57.

this bond energy is almost 10-fold lower than typical Pt–C σ-bond energies mentioned above. Nevertheless, this weak value exceeds DFT periodic-slab calculations of these bond energies[58] by almost 100%, as shown in Fig. 7. The large errors in DFT seen here are at least partially due to the relatively larger role played by London dispersion forces in benzene and naphthalene adsorption,[57] since these are not treated fully by DFT. Interestingly, the adsorption energy for di-σ-C_6H_{10} on Pt(111) was predicted by the same DFT method to be 112 kJ mol^{-1},[58] within 8% of the measured integral heat of adsorption at this same coverage of 122 kJ mol^{-1} from SCAC given above. This implies that DFT is capable of calculating very reliable adsorption energies for hydrocarbons with bonding dominated by strong Pt–C σ-bonds; however, weaker π-bonded systems, such as benzene on Pt(111), or systems with large contributions from Van der Waals interactions, remain a challenge for DFT, and the accuracy is poor.

Acknowledgements

The authors acknowledge support for this work by the National Science Foundation under CHE-0757221 and the Department of Energy Office of Basic Energy Sciences, Chemical Sciences Division. We thank many past group members for important contributions to this work, and gratefully acknowledge John W. Heutink and Brian P. Holm of the Chemistry Department machine shop and James A. Gladden for their invaluable skill and expertise. Finally, CTC sincerely thanks Prof. Dr Gerhard Ertl for mentoring his scientific development as a postdoctoral researcher back in 1979–1980, for his inspirational leadership, and for his kind support, both scientific and personal, throughout his life.

References

1 D. Brennan, D. O. Hayward and B. M. W. Trapnell, *Proc. R. Soc. London, Ser. A*, 1960, **A256**, 81–105.
2 S. Černý, *Surf. Sci. Rep.*, 1996, **26**, 1–59.
3 G. Ertl, *Angew. Chem., Int. Ed.*, 2008, **47**, 2–14.
4 G. Ertl, *Catal. Rev. Sci. Eng.*, 1980, **21**, 201–223.
5 C. T. Campbell, G. Ertl, H. Kuipers and J. Segner, *J. Chem. Phys.*, 1980, **73**, 5862–5873.
6 G. A. Somorjai, *Introduction to Surface Chemistry and Catalysis*, Wiley-Interscience, New York, 1994.
7 D. A. Kyser and R. I. Masel, *Rev. Sci. Instrum.*, 1987, **58**, 2141–2144.
8 C. E. Borroni-Bird, N. Al-Sarraf, S. Andersson and D. A. King, *Chem. Phys. Lett.*, 1991, **183**, 516–520.
9 N. Al-Sarraf and D. A. King, *Surf. Sci.*, 1994, **307–309**, 1–7.
10 A. Stuck, C. E. Wartnaby, Y. Y. Yeo and D. A. King, *Phys. Rev. Lett.*, 1995, **74**, 578–581.
11 J. T. Stuckless, N. Al-Sarraf, C. Cartnaby and D. A. King, *J. Chem. Phys.*, 1993, **99**, 2202–2112.
12 A. Stuck, C. E. Wartnaby, Y. Y. Yeo, J. T. Stuckless, N. Al-Sarraf and D. A. King, *Surf. Sci.*, 1996, **349**, 229–240.
13 W. A. Brown, R. Kose and D. A. King, *Chem. Rev.*, 1998, **98**, 797–831.
14 L. Vattuone, Y. Y. Yeo and D. A. King, *J. Chem. Phys.*, 1996, **104**, 8096–8102.
15 Y. Y. Yeo, A. Stuck, C. E. Wartnaby, R. Kose and D. A. King, *J. Mol. Catal. A: Chem.*, 1998, **131**, 31–38.
16 Y. Y. Yeo, L. Vattuone and D. A. King, *J. Chem. Phys.*, 1997, **106**, 392–401.
17 A. D. Karmazyn, V. Fiorin and D. A. King, *Surf. Sci.*, 2003, **547**, 184–192.
18 W. A. Brown, R. Kose and D. A. King, *Surf. Sci.*, 1999, **440**, 271–278.
19 R. Kose, W. A. Brown and D. A. King, *Surf. Sci.*, 1998, **404**, 856–860.
20 J. T. Stuckless, D. E. Starr, D. J. Bald and C. T. Campbell, *J. Chem. Phys.*, 1997, **107**, 5547.
21 J. T. Stuckless, N. A. Frei and C. T. Campbell, *Rev. Sci. Instrum.*, 1998, **69**, 2427–2438.
22 J. T. Stuckless, N. A. Frei and C. T. Campbell, *Sens. Actuators, B*, 2000, **62**, 13–22.
23 D. E. Starr and C. T. Campbell, *J. Phys. Chem. B*, 2001, **105**, 3776–3782.
24 H. M. Ajo, H. Ihm, D. E. Moilanen and C. T. Campbell, *Rev. Sci. Instrum.*, 2004, **75**, 4471–4480.
25 S. F. Diaz, J. F. Zhu, N. Shamir and C. T. Campbell, *Sens. Actuators, B*, 2005, **107**, 454–460.
26 O. Lytken, W. Lew, J. J. W. Harris, E. K. Vestergaard, J. M. Gottfried and C. T. Campbell, *J. Am. Chem. Soc.*, 2008, **130**, 10247–10257.
27 S. J. Dixon-Warren, M. Kovar, C. E. Wartnaby and D. A. King, *Surf. Sci.*, 1994, **307**, 16–22.
28 J. A. Rodriguez and C. T. Campbell, *J. Phys. Chem.*, 1989, **93**, 826–835.
29 J. A. Rodriguez and C. T. Campbell, *J. Catal.*, 1989, **115**, 500–520.
30 F. C. Henn, A. L. Diaz, M. E. Bussell, M. B. Hugenschmidt, M. E. Domagala and C. T. Campbell, *J. Phys. Chem.*, 1992, **96**, 5965–5974.
31 M. E. Bussell, F. C. Henn and C. T. Campbell, *J. Phys. Chem.*, 1992, **96**, 5978–5982.
32 D. P. Land, C. L. Pettiette-Hall, R. T. McIver, Jr. and J. C. Hemminger, *J. Am. Chem. Soc.*, 1989, **111**, 5970–5972.
33 C. L. Pettiette-Hall, D. P. Land, R. T. McIver, Jr. and J. C. Hemminger, *J. Am. Chem. Soc.*, 1991, **113**, 2755–2756.
34 D. P. Land, W. Erley and H. Ibach, *Surf. Sci.*, 1993, **289**, 237–246.
35 J. M. Campbell, S. G. Seimanides and C. T. Campbell, *J. Phys. Chem.*, 1989, **93**, 815–826.
36 H. Ihm, H. M. Ajo and C. T. Campbell, *J. Phys. Chem. B*, 2004, **108**, 14627–14633.
37 *CRC Handbook of Chemistry and Physics (Internet Version)*, ed. D. R. Lide, CRC Press/Taylor and Francis, Boca Raton, FL, 2008.
38 P. R. Norton, J. A. Davies and T. E. Jackman, *Surf. Sci.*, 1982, **P121**, 103–110.
39 B. E. Nieuwenhuys, *Surf. Sci.*, 1976, **59**, 430–446.
40 B. Poelsema, G. Mechtersheimer and G. Comsa, *Surf. Sci.*, 1981, **111**, 519–544.
41 B. J. J. Koeleman, S. T. de Zwart, A. L. Boers, B. Poelsema and L. K. Verhey, *Nucl. Instrum. Methods Phys. Res.*, 1983, **218**, 225–229.
42 S. L. Tait, Z. Dohnalek, C. T. Campbell and B. D. Kay, *J. Chem. Phys.*, 2005, **122**, 164708.
43 S. L. Tait, Z. Dohnalek, C. T. Campbell and B. D. Kay, *J. Chem. Phys.*, 2006, **125**, 234308.
44 O. V. Dorofeeva, L. V. Gurvich and V. S. Jorish, *J. Phys. Chem. Ref. Data*, 1986, **15**, 437–464.
45 S. S. Chen, R. C. Wilhoit and B. J. Zwolinski, *J. Phys. Chem. Ref. Data*, 1975, **4**, 859–870.
46 D. H. Parker, C. L. Pettiette-Hall, Y. Z. Li, R. T. McIver, Jr. and J. C. Hemminger, *J. Phys. Chem.*, 1992, **96**, 1888–1894.
47 C. T. Campbell, J. M. Campbell, P. J. Dalton, F. C. Henn and S. G. Seimanides, *J. Phys. Chem.*, 1989, **93**, 806–814.
48 J. M. Campbell and C. T. Campbell, *Surf. Sci.*, 1989, **210**, 46–68.
49 F. C. Henn, P. J. Dalton and C. T. Campbell, *J. Phys. Chem.*, 1989, **93**, 836–846.
50 C. T. Campbell, *Annu. Rev. Phys. Chem.*, 1990, **41**, 775–837.
51 C. T. Campbell, Y.-K. Sun and W. H. Weinberg, *Chem. Phys. Lett.*, 1991, **179**, 53–57.
52 M. Saeys, M.-F. Reyniers, M. Neurock and G. B. Marin, *Surf. Sci.*, 2006, **600**, 3121–3134.
53 H. E. Bryndza, L. K. Fong, R. A. Paciello, W. Tam and J. E. Bercaw, *J. Am. Chem. Soc.*, 1987, **109**, 1444–1456.
54 H. Gross, C. T. Campbell and D. A. King, *Surf. Sci.*, 2004, **572**, 179–190.
55 M. A. Newton and C. T. Campbell, *Catal. Lett.*, 1996, **37**, 15–23.
56 D. F. McMillen and D. M. Golden, *Annu. Rev. Phys. Chem.*, 1982, **33**, 493–532.
57 J. M. Gottfried, E. K. Vestergaard, P. Bera and C. T. Campbell, *J. Phys. Chem. B*, 2006, **110**, 17539–17545.
58 C. Morin, D. Simon and P. Sautet, *Surf. Sci.*, 2006, **600**, 1339–1350.